Incorporating Spatial Variability into Geotechnical Reliability-based Design

Draft report for the joint TC205/TC304 discussion group "Incorporating spatial variability into geotechnical reliability-based design", prepared by Dian-Qing Li

Lead discusser: Dian-Qing Li

Discussers (alphabetic order): Zi-Jun Cao, Satyanarayana Murty Dasaka, Jin-Song Huang, Mark Jaksa, Shin-ichi Nishimura, Armin Stuedlein, Giovanna Vessia

INTRODUCTION

Geotechnical materials are natural materials. Their properties are affected by various factors in natural geological processes, such as parent materials, weathering and erosion processes, transportation agents, conditions of sedimentation, etc. (e.g., Mitchell and Soga, 2005). These factors vary spatially from one location to another, which subsequently lead to inherent spatial variability (ISV) of geotechnical properties (Vanmarcke, 2010). ISV has been considered as a major source of uncertainties in soil properties (e.g., Christian et al., 1994; Kulhawy, 1996; Phoon and Kulhawy, 1999a; Baecher and Christian, 2003; Wang et al., 2016). It significantly affects the safety (measured by factor of safety, FS) and reliability (measured by probability of failure, P_f, or reliability index, β) of geotechnical structures, such as foundations (e.g., Fenton and Griffiths, 2002, 2003 and 2007; Wang and Cao, 2013; Li et al., 2015a), retaining structures (e.g., Fenton and Griffiths, 2005), and slopes (e.g., Griffith and Fenton, 2004, 2009; Huang et al., 2010; Wang et al., 2011; Li et al., 2014; Jiang et al., 2014; Li et al., 2016a; Xiao et al., 2016). ISV shall, hence, be rationally taken into account in geotechnical designs, which constitutes a major difference in reliability-based designs (RBD) of geotechnical structures and building structures.

ISV can be explicitly modeled in geotechnical RBD using random field theory (Vanmarcke, 2010). Figure 1 shows major steps for incorporating ISV in geotechnical RBD based on random field theory. In general, it starts with probabilistic *characterization* of ISV based on site investigation data (e.g., in-situ/laboratory test results) and site information available prior to the project (namely prior knowledge), which determines statistical information of geotechnical design parameters, including spatial trend, statistics (e.g., mean and standard deviation), and correlation functions. Such information is needed as input for *modeling* ISV in geotechnical RBD, which represents or simulates ISV of geotechnical design parameters using random fields with pre-defined statistical information. Here, the authors need to emphasize that this report focuses on *modeling* ISV in geotechnical RBD based on known/assumed statistical information of geotechnical parameters, and will not discuss probabilistic *characterization* of ISV, i.e., how to derive statistical information from site investigation data and prior knowledge. Relevant studies on probabilistic characterization of ISV of geotechnical parameters are referred to DeGroot and Baecher (1993), Jaksa (1995), Fenton et al. (1999a,b), Uzielli

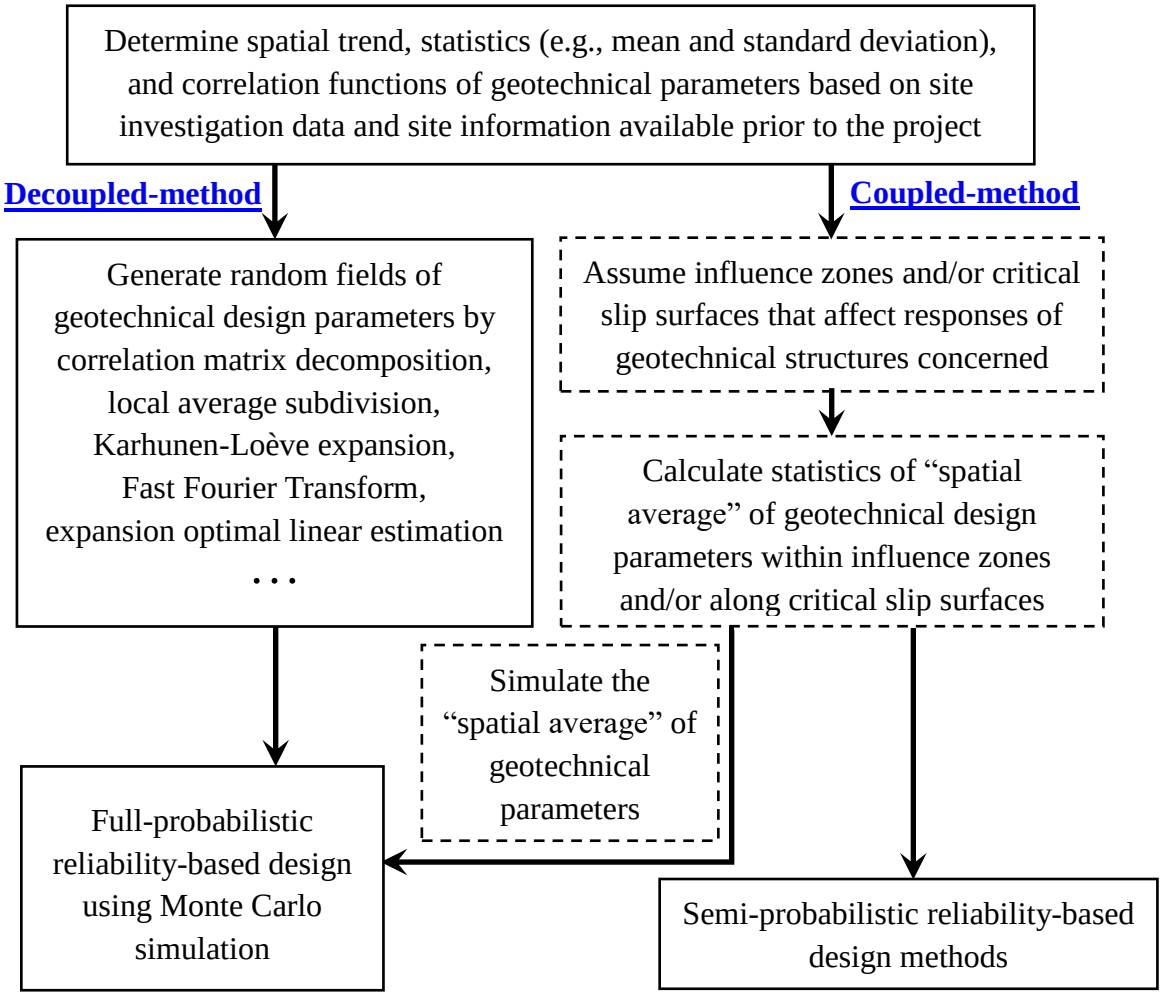

Figure 1 Incorporating spatial variability into geotechnical RBD based on random field theory.

et al. (2005), Wang et al., (2010), Dasaka and Zhang (2012), Stuedlein et al. (2012), Cao and Wang (2013, 2014), Firouzianbandpey et al. (2014, 2015), Ching et al., (2015), Cao et al., (2016), Wang et al. (2016), and Tian et al. (2016).

Based on random field theory, there are generally two ways to model ISV in geotechnical RBD, which are named as decoupled (D)-method and coupled (C)-method in this report. As shown in Figure 1, D-method directly simulates random fields of geotechnical design parameters based on their statistical information derived from site investigation *without* considering influence zones and/or critical slip surfaces that affect responses (e.g., resistance moment, bearing capacity, and settlement, etc.) of geotechnical structures concerned. With the D-method, a number of random field realizations of geotechnical parameters can be directly generated under a full-probabilistic RBD framework using Monte Carlo simulation (MCS) (e.g., Cao et al., 2013; Wang and Cao, 2013; Cao and Wang, 2014; Li et al., 2016b). Then, each random field realization is used as input of deterministic geotechnical model to predict responses of geotechnical structures concerned in design. By this means, ISV modeling is deliberately *decoupled* from deterministic analyses of geotechnical structures. This provides flexibility in choosing different deterministic geotechnical models (e.g., limit equilibrium

method and finite element method) and allows searching for critical slip surfaces and determining influences zones of soil masses affecting responses of geotechnical structures. For example, D-method is applied in random finite element method to model ISV for geotechnical probabilistic analysis and risk assessment (e.g., Griffith and Fenton, 2004, 2009; Huang et al., 2010, 2013; Li et al., 2016a, Xiao et al., 2016), in which ISV modeling does not involve information on geotechnical failure mechanisms or influence zones.

In contrast, C-method uses random field theory to calculate statistics of spatial averages of geotechnical design parameters within influence zones and/or along critical slip surfaces affecting responses of geotechnical structures (Vanmarcke, 1977; El-Ramly et al., 2002, 2005; Zhang and Chen, 2012; Wang and Cao, 2013). The spatial average of geotechnical design parameters over a spatial curve (e.g., slip surfaces) or area (e.g., influence zones) has the same mean as geotechnical design parameters at a "point" that is directly simulated in D-method, but its variance is reduced due to spatial averaging. The extent of reduction in variance is quantified by variance reduction function Γ^2 that is defined as a ratio of the variance of the spatial average over the variance of geotechnical design parameters at a "point" (Vanmarcke, 2010). Calculating Γ^2 requires geometric information (e.g., location and length) of influence zones and/or critical slip surfaces. Such information is, however, unknown prior to geotechnical deterministic analyses and shall be assumed for calculating statistics of spatial averages of geotechnical design parameters in C-method. Hence, using C-method in geotechnical RBD, ISV modeling is *coupled* with geotechnical deterministic analyses. After statistics of spatial averages of geotechnical design parameters are calculated, they can either be used to determine characteristic values of geotechnical design parameters for semi-probabilistic RBD approaches (e.g., Eurocode 7 (Orr, 2015)) or be applied to simulating spatial averages within pre-defined influence zones and/or along assumed critical failure surfaces under a full-probabilistic RBD framework (El-Ramly, 2002, 2006; Wang and Cao, 2013).

C-method uses spatial averages of geotechnical design parameters as their corresponding estimates along critical slip surfaces or within influence zones. However, the spatial average might not be the same as "mobilized" values of geotechnical parameters that control responses of geotechnical structures concerned in designs, which has been demonstrated under simple stress states (e.g., Ching and Phoon, 2012, 2013; Ching et al., 2014). Hence, compared with direct and rigorous modeling of ISV using D-method, C-method is an indirect and approximate way to model ISV in geotechnical RBD. How such an indirect and approximate modeling of ISV affects RBD of real geotechnical structures is unclear. This issue is systematically explored for different geotechnical structures, including drilled shaft, sheet pile wall, and soil slope, in this report. In addition, Γ^2 is needed for implementing C-method. It can be calculated exactly according to correlation functions of geotechnical design parameters, or be evaluated approximately by a simplified formulation to bypass the need of determining correlation functions. This report will also discuss effects of different ways to calculate Γ^2 on geotechnical RBD.

PROBABILISTIC MODELING OF SPATIAL VARIABILITY IN GEOTECHNICAL RBD

As shown in Figure 1, both D-method and C-method can be applied to modeling ISV in full-probabilistic RBD approach using MCS. To enable a consistent comparison, this report adopts a recently developed MCS-based RBD approach, so-called the expanded RBD approach, to perform RBD of geotechnical structures with D-method and C-method, respectively. The expanded RBD approach formulates the design process as a systematic sensitivity analysis on possible designs in design space (e.g., a possible range of drilled shaft length) defined by geotechnical engineers, in which P_f values of all the possible designs are calculated by a single run of MCS. Then, the final design is determined according to target reliability levels and economic requirement. Details of algorithms and implementation procedures of the expanded RBD approach are referred to Wang (2011), Wang et al. (2011), Wang and Cao (2013, 2015), and Li et al. (2016b).

The expanded RBD approach provides flexibility of modeling ISV in different ways for geotechnical RBD, such as D-method and C-method. Based on the expanded RBD approach, this report aims to preliminarily reveal effects of indirect and approximate ISV modeling through C-method on geotechnical RBD and probabilistic analysis by comparing respective RBD results and/or reliability estimates (e.g., P_f) that are obtained using D-method and C-method, and to demonstrate effects of different ways to calculate Γ^2. For the illustration and simplification, only one-dimensional (1-D) ISV of geotechnical parameters is considered in this report. The following two subsections describe 1-D ISV modeling using D-method and C-method, respectively.

Decoupled modeling by random field simulation (D-method)

D-method models ISV of geotechnical parameters in a direct and explicit manner. Consider, for example, a geotechnical design parameter X (e.g., effective friction angle ϕ') in a statistically homogenous soil layer. As shown in Figure 2, the ISV of X with depth (or in some direction) can be characterized by a 1-D homogenous lognormal random field $\underline{X(z_i)}$, in which z_i is a spatial coordinate (e.g., depth in the vertical direction) of the i-th location and X is a lognormal random variable with a mean μ and standard deviation σ (or coefficient of variation $COV_X = \sigma/\mu$). In the context of random fields, the spatial correlation between variations of X at different locations is characterized by the scale of fluctuation and correlation function (Vanmarcke, 1977 and 2010). Here, the correlation function is taken as a single exponential correlation function, and the correlation coefficient ρ_{ij} between the logarithms [e.g., $\ln X(z_i)$ and $\ln X(z_j)$] of X at i-th and j-th locations is given by:

$$\rho_{ij} = \exp(-2|\Delta D_{i,j}|/\lambda) \quad (1)$$

where λ = scale of fluctuation; $|\Delta D_{i,j}|$ = the distance between i-th and j-th locations. For a given set of statistics (including μ, σ, and λ) and correlation function, the statistically homogenous random field $\underline{X}$ of X can be generated using various simulation techniques, such as correlation matrix decomposition (e.g., Wang et al., 2011; Li et al., 2015b, 2016a), local average subdivision (e.g.,

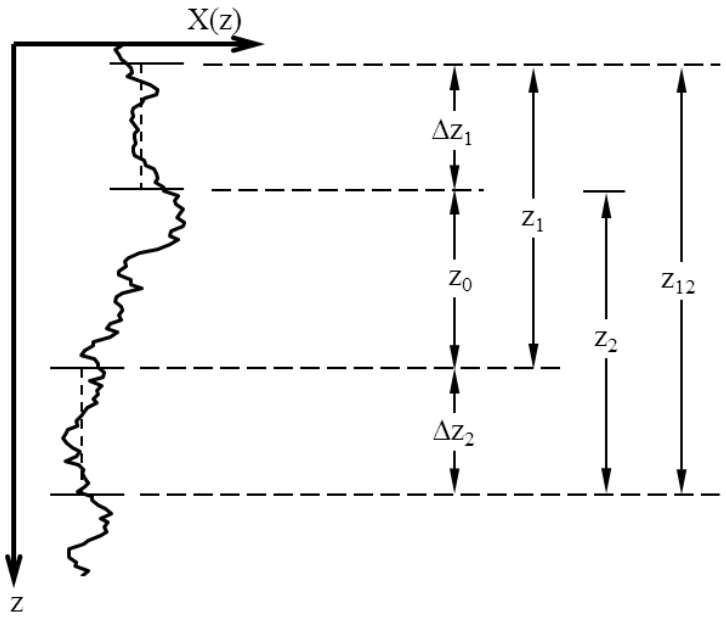

Figure 2 Illustration of 1-D spatial variability.

Fenton and Vanmarcke 1990; Fenton and Griffiths, 2008), Karhunen-Loève expansion (e.g., Phoon et al. 2002; Cho 2010; Jiang et al. 2015), expansion optimal linear estimation (e.g., Li and Der Kiureghian, 1993; Xiao et al., 2016). Consider, for example, using the covariance matrix decomposition method to simulate $\underline{X}$ in this report, by which X can be written as:

$$\underline{\ln X} = \mu_{\ln X}\underline{1} + \sigma_{\ln X}\underline{L}^{T}\underline{\varepsilon} \tag{2}$$

where $\mu_{\ln X} = \ln\mu - \sigma^2_{\ln X}/2$ and $\sigma_{\ln X} = \sqrt{\ln[1+(\sigma_X/\mu_X)^2]}$ are the mean and standard deviation of the logarithm (i.e., lnX) of X, respectively; $\underline{1}$ = a vector with N_t components that are all equal to one; $\underline{\varepsilon} = [\varepsilon_1,\ldots,\ \varepsilon_{Nt}]^T$ = a standard Gaussian vector with N_t independent components; $\underline{L}$ = a N_t -by- N_t upper-triangular matrix obtained by Cholesky decomposition of the correlation matrix $\underline{R}$ satisfying

$$\underline{R} = \underline{L}^{T}\underline{L} \tag{3}$$

and the (i, j)-th entry of $\underline{R}$ is given by the correlation function, e.g., Eq. (1). Using Eqs. (1)-(3), the ISV of X is explicitly simulated and is used as input in subsequent deterministic analysis of geotechnical structures to evaluate their responses (e.g., resistance moment, bearing capacity, and settlement, etc.) concerned in RBD. Note that little information on deterministic model of geotechnical structures is involved in Eqs. (1)-(3), making the ISV simulation using D-method be decoupled from the geotechnical deterministic analysis.

Coupled modeling by spatial average technique (C-method)

In C-method, the geotechnical design parameter X over a depth interval (e.g., influence zones) or along a spatial curve (e.g., critical slip surface of slope stability) is characterized by a single random variable $X_{\Delta z}$ that represents the spatial average of X over the depth interval or along the spatial

curve and has a reduced variance due to spatial averaging (e.g., Vanmarcke, 1977; Griffiths and Fenton, 2004; Wang and Cao, 2013). Let Δz denote the length of the depth interval or the spatial curve. Due to the spatial averaging over Δz, the variance of the equivalent normal random variable $\ln X$ of X is reduced, and the variance reduction of $\ln X$ is described by a variance reduction function $\Gamma^2_{\Delta z}$ in C-method. For example, $\Gamma^2_{\Delta z}$ for the single exponential correlation function given by Eq. (1) is calculated as (Vanmarcke, 2010)

$$\Gamma^2_{\Delta z} = [\lambda/(2\Delta z)]^2[2(2\Delta z/\lambda - 1 + \exp(-2\Delta z/\lambda))] \quad (4)$$

Note that calculation of $\Gamma^2_{\Delta z}$ depends on the correlation function. For exact evaluation of $\Gamma^2_{\Delta z}$, the correlation function is hence needed. This is a non-trivial task in geotechnical design practice because proper determination of the correlation function requires a large amount of geotechnical data that is usually not available at a specific site for routine geotechnical designs. Based on a limited number of geotechnical data obtained from site investigation, the most probable correlation function can be selected from a pool of candidates using Bayesian approaches (Cao and Wang, 2014, Tian et al., 2016).

Alternatively, to avoid determining the correlation function, $\Gamma^2_{\Delta z}$ can be approximate as (e.g., Vanmarcke, 2010)

$$\Gamma^2_{\Delta z} = \begin{cases} 1 & \Delta z < \lambda \\ \lambda/\Delta z & \Delta z > \lambda \end{cases} \quad (5)$$

Eq. (5) gives a simplified form of the variance reduction function to conveniently calculate the variance reduction factor for various correlation structures, and it is valid for different correlation functions (Vanmarcke, 1977). Using Eq. (5) in C-method avoids determining the correlation function of geotechnical parameters. It is widely used in geotechnical literature (e.g., Vanmarcke, 1977; Phoon and Kulhawy, 1999b; El-Ramly et al., 2002; Wang and Cao, 2013). Figure 3 shows variance reduction functions given by Eqs. (4) and (5) by a solid line and a dashed line, respectively. The difference between the two variance functions is also plotted in Figure 3 by a dotted line. It is shown that the difference increases as $\Delta z/\lambda$ increases from 0 to 1 and then decreases as $\Delta z/\lambda$ increases further. The maximum difference occurs as $\Delta z/\lambda = 1$. Effects of using the approximate variance reduction function on geotechnical designs will be discussed later in this report.

Moreover, the geotechnical deterministic model may involve more than one spatial average of X over different sections (e.g., two depth intervals), which are spatially correlated. Let Δz_1 and Δz_2 denote the respective lengths of spatial average sections. When using C-method to model 1-D ISV,

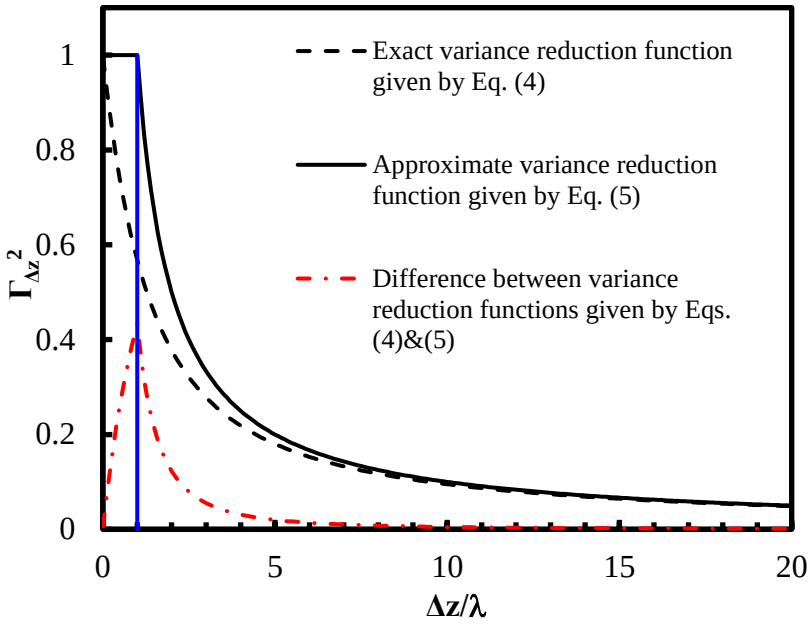

Figure 3 Comparison of variance reduction functions given by Eqs. (4) and (5).

the spatial correlation between spatial averages of X over Δz_1 and Δz_2 is calculated as:

$$\rho_A = \frac{z_0^2\Gamma_{z_0}^2 - z_1{}^2\Gamma_{z_1}^2 - z_2^2\Gamma_{z_2}^2 + z_{12}^2\Gamma_{z_{12}}^2}{2\Delta z_1\Delta z_2\sqrt{\Gamma_{\Delta z_1}^2\Gamma_{\Delta z_2}^2}} \tag{6}$$

where z_0 = separation distance between the two spatial average sections; z_1= the distance from the beginning of the first section to the beginning of the second section; z_{12} = the distance from the beginning of the first section to the end of the second section; and z_2 = the distance from the end of the first section to the end of the second section. $\Gamma_{z_0}^2$, $\Gamma_{z_1}^2$, $\Gamma_{z_2}^2$, $\Gamma_{z_{12}}^2$, $\Gamma_{\Delta z_1}^2$, and $\Gamma_{\Delta z_2}^2$ = the respective variance reduction factors of $\ln X$ due to the spatial averaging over z_0, z_1, z_2, z_{12}, Δz_1 and Δz_2, which are illustrated in Figure 1.

Note that Eqs. (4)-(6) need the length of spatial average sections (e.g., influence zones for side resistance of drilled shafts and the critical slip surface of slope stability) as input information, which depends on geotechnical deterministic models. Determining proper spatial average sections is pivotal to calculating the variance reduction function in C-method. Hence, C-method couples the ISV modeling and geotechnical deterministic analyses, and it incorporates ISV into geotechnical design in an indirect and approximate manner. Effects of using C-method to model ISV on geotechnical designs can be evaluated by comparing the design results or reliability estimates (e.g., P_f) that are obtained using D-method and C-method, respectively. This is discussed based on three geotechnical examples (including a drilled shaft example, a sheet pile wall example, and a soil slope example) in the following three sections.

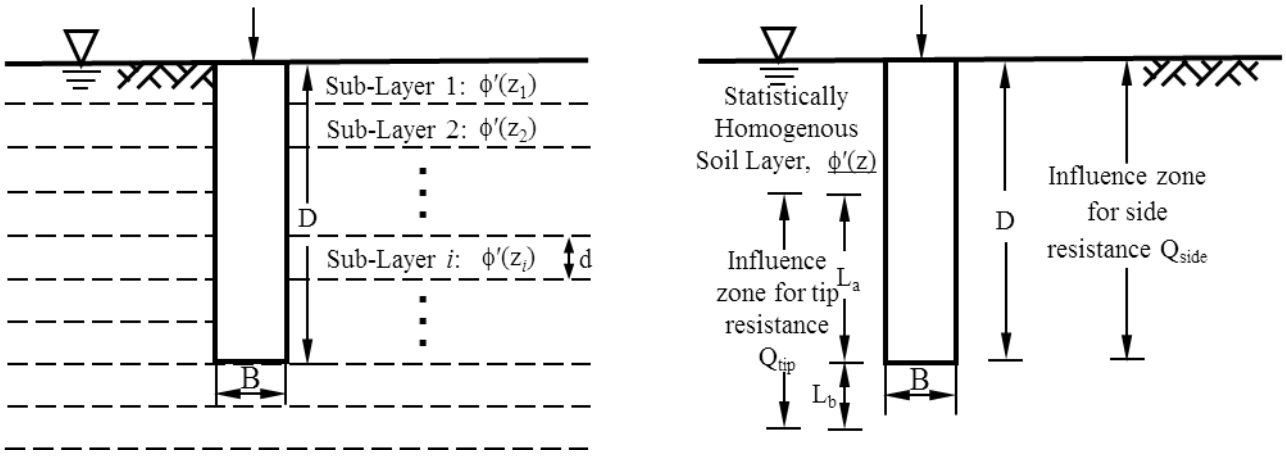

(a) Random field simulation of ϕ'

(b) Influence zones for side resistance Q_{side} and tip resistance Q_{tip}

Figure 4 Illustration of spatial variability modeling using D-method (see 4(a)) and C-method (see 4(b)) in drilled shaft designs

ILLUSTRATIVE EXAMPLE I: DRILLED SHAFT

To explore effects of indirect and approximate modeling of ISV on foundation designs, this section redesigns a drilled shaft example using the expanded RBD approach together with D-method and C-method to model ISV, respectively. As shown in Figure 4, the drilled shaft is installed in loose sand with a total unit weight $\gamma = 20.0$ kN/m^3 and mean effective stress friction angle $\mu_{\phi'} = 32^o$. The shaft is assumed to fail in drained general shear under a design compression load $F_{50} = 800$ kN with an allowable displacement $y_a = 25$ mm. The key design parameters in this example are the drilled shaft diameter B and depth D, which are required to support the design compression load and to have a shaft displacement less than 25 mm.

The expanded RBD approach is used to determine the minimum feasible design value (i.e., D_{min}) of D for a given B value. For comparison, D-method and C-method are applied to modeling ISV of ϕ', leading to different design results through the expanded RBD approach. In D-method, Eqs. (1)-(3) are used to directly simulate the random field of ϕ' in the sand layer (see Figure 4(a)), where λ varies from 0.2 to 1000m. In contrast, ϕ' in the sand layer surrounding the drilled shaft is modeled by ϕ'_{side} and ϕ'_{tip} in C-method, which represent the respective spatial averages of ϕ' over influence zones for evaluating side resistance Q_{side} and tip resistance Q_{tip}. As shown in Figure 4(b), the influence zone of Q_{side} is taken as the depth interval from ground surface to the tip and its length is equal to shaft depth D. The influence zone of Q_{tip} is taken as a depth interval from L_a (e.g., min{8B,D}) above the tip to L_b (e.g., 3.5B) below the tip, and its maximum length is D_{max}+3.5B for a given B, where D_{max} is the maximum possible value of the shaft depth and is taken as 10m in this example. Note that the locations and lengths of influence zones for evaluating Q_{side} and Q_{tip} shall be specified in C-method (see Eqs. (4)-(6)) prior to the design, which depends on the deterministic analysis model used in design. More details of modeling and calculations of the drilled shaft example are referred to Wang and Cao (2013).

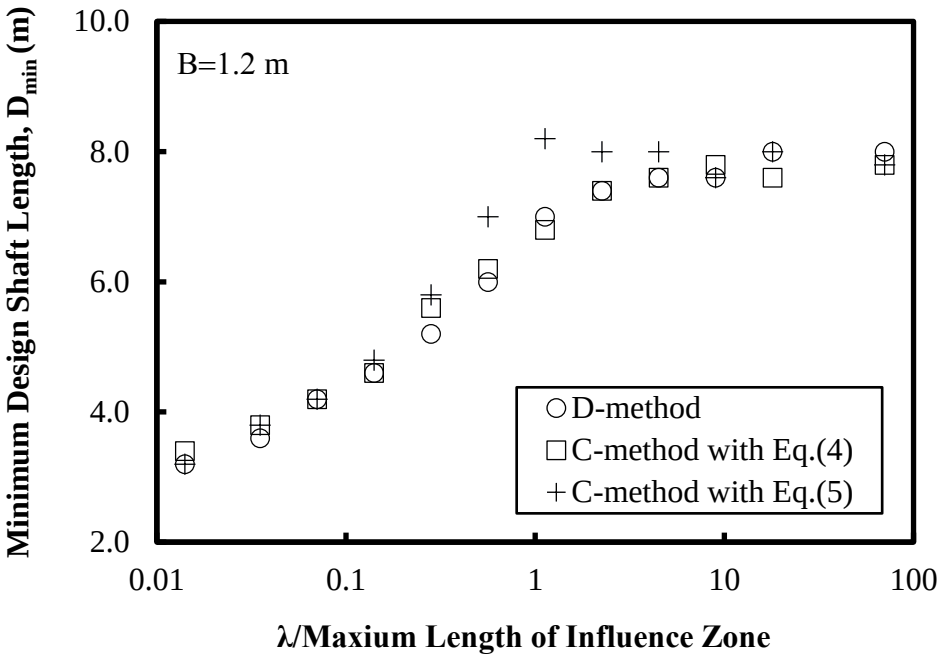

Figure 5 Comparison of drilled shaft design results using D-method and C-method in expanded RBD for B = 1.2m

Figure 5 shows the variation of D_{min} for B = 1.2m obtained using the expanded RBD approach with D-method as a function of normalized λ by circles. For each value of normalized λ, Figure 5 also includes D_{min} values obtained using C-method with the exact form (i.e., Eq. (4)) and the approximate form (i.e., Eq. (5)) of variance reduction function by squares and crosses, respectively. The D_{min} values here are determined according to the target failure probability p_T = 0.0047 for serviceability limit state, which has been shown to control the design in this example (Wang and Cao, 2013). As shown in Figure 5, for a given value of normalized λ , the circle generally plots closely to the squares. The results obtained using the C-method with the exact form of variance reduction function agree well with those obtained using D-method. This indicates that the spatial average of ϕ' represents "mobilized" value of ϕ' over the influence zones for drilled shaft resistance reasonably well in this example. Such an observation is further confirmed by comparing the side resistance estimated from realizations of ϕ' random field in D-method and their corresponding spatial averages of ϕ' over the shaft depth, as shown in Figure 6.

Figure 5 also compares design results obtained from C-method with the exact form (i.e., Eq. (4)) and the approximate form (i.e., Eq. (5)) of variance reduction function. As λ is smaller than one tenth of the maximum length L_{max} (i.e., D_{max}+3.5B in this example) of influence zone for drilled shaft resistance or greater than ten times of L_{max}, using Eqs. (4) and (5) gives similar design results. However, when λ is close to L_{max}, there is apparent difference between the two set of design results. Such a difference is attributed to approximation in variance reduction function. As shown in Figure 3, the maximum difference between variance reduction functions given by Eqs. (4) and (5) occurs as

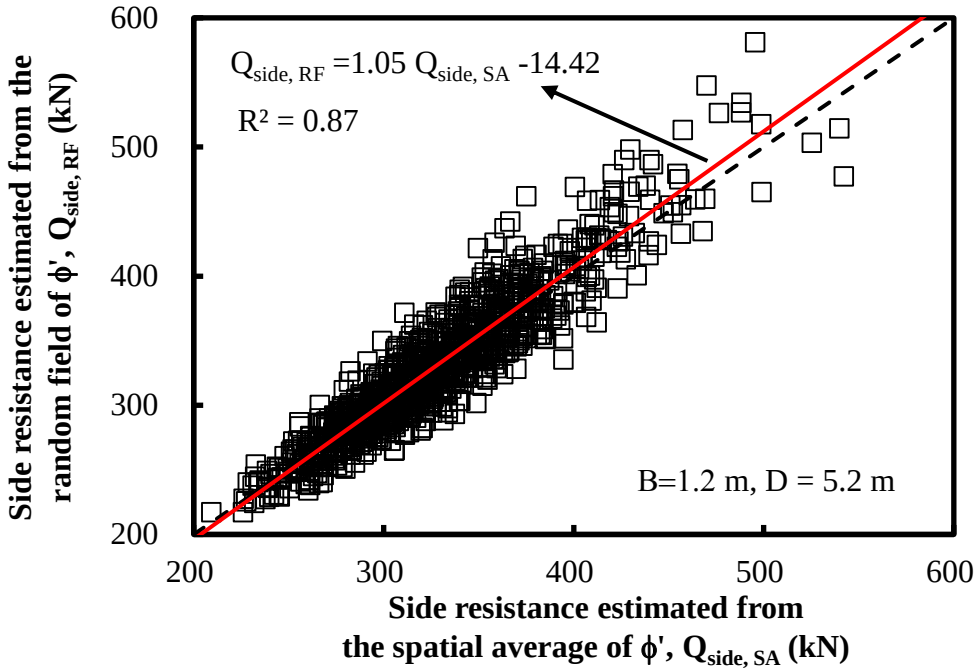

Figure 6 Comparison of side resistance calculated from realizations of ϕ' random fields and their corresponding spatial averages over influence zones for the design with B = 1.2m and D=5.2m

λ is equal to the length of spatial average interval, e.g., L_{max} in this example. Hence, when the length of influence zone is close to λ adopted in design, the approximate variance reduction function given by Eq. (5) shall be used with caution.

ILLUSTRATIVE EXAMPLE II: SHEET PILE WALL

For further illustration, this section redesigns an embedded sheet pile wall example using the expanded RBD approach together with D-method and C-method to model ISV in design, respectively. As shown in Figure 7, the embedded sheet pile wall is designed for a 3-m deep excavation, and is installed in a sand layer, where the total unit weight of sand is 20 kN/m^3 and effective friction angle ϕ' (i.e., lnX in Eq. (2)) of sand is normally distributed with a mean of 39° and a standard deviation of 3.9°. The ground water levels are at the ground surface in front of the wall and at the depth of 1.5m behind the wall. In addition, the surcharge q behind the wall is considered as a variable load, which is normally distributed and has a mean of 8.02 kPa and a standard deviation of 1.20 kPa. The aim of the sheet pile wall design example is to find an embedded depth d that satisfies the moment equilibrium about point O and to determine an additional embedded depth Δd by solving the horizontal force equilibrium equation (Wang, 2013). For simplification, Δd is commonly taken as 0.2d, which often leads to conservative designs (e.g., Craig, 2004; Wang, 2013; Li et al., 2016b). Then, the required depth D_{spw} of the sheet pile wall example is equal as 1.2d, and it ranges from 1m to 8m with an increment of 0.1m. For a given D_{spw} value, d (i.e., D_{spw}/1.2) and Δd (i.e., 0.2d) are calculated, and the net resistance moment M_R about point O provided by passive earth pressure is evaluated, as well as the net overturning moment M_O resulted from the active pressure acting. After that, the FS is obtained, details of which are referred to Craig (2004) and Wang (2013).

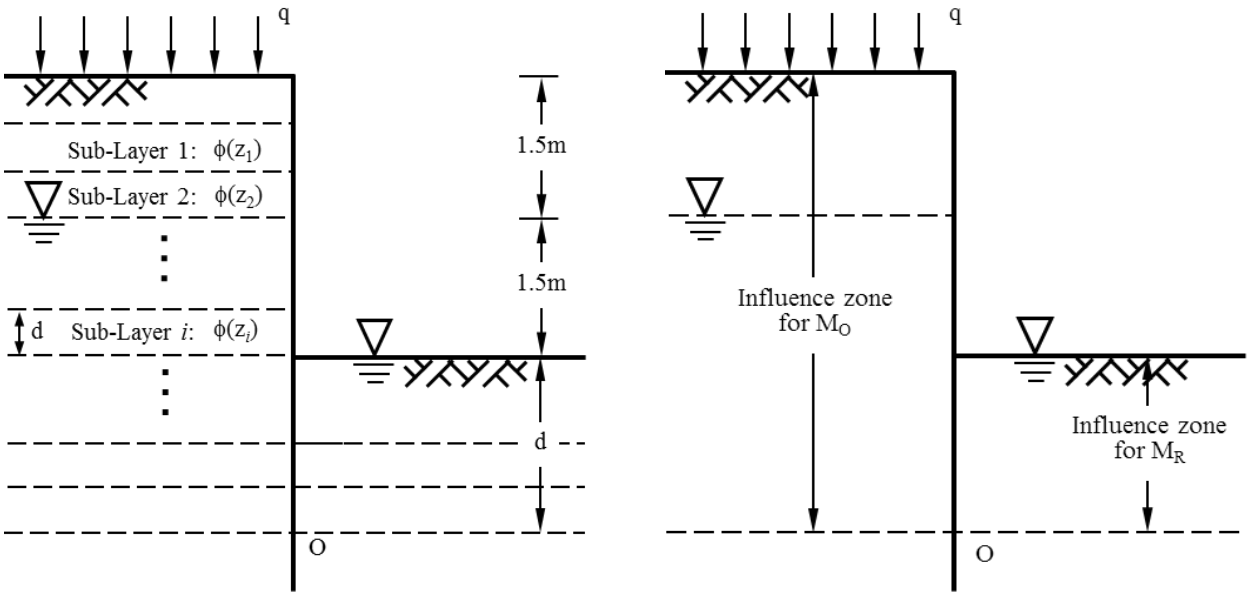

(a) Random field simulation of ϕ'

(b) Influence zones for resistance and overturning moments

Figure 7 Illustration of spatial variability modeling using D-method (see 7(a))and C-method (see 7(b)) in sheet pile wall designs

The expanded RBD approach is used to determine the minimum feasible design value (i.e., D_{min}) of D_{swp}. Similar to the drilled shaft design, D-method and C-method are applied to modeling ISV of ϕ' in the sand layer in expanded RBD. In D-method, Eqs. (1)-(3) are used to directly simulate the random field of ϕ' in the sand layer (see Figure 7(a)), where λ varies from 0.2 m to 1000 m. In contrast, ϕ' in the sand layer surrounding the sheet pile wall is modeled by ϕ'_O and ϕ'_R in C-method, which represent the respective spatial averages of ϕ' over influence zones for evaluating M_O and M_R. As shown in Figure 7(b), the influence zone of M_R is taken as the depth interval from ground surface in front of the wall to point O, and its length is equal to d minus over-digging depth(0.3m); the influence zone of M_O is taken as a depth interval from ground surface behind the wall to point O, and its maximum length is d_{max}+3.0m for a given B, where d_{max} is the maximum possible value of the embedded depth and is taken as 8.0/1.2 = 6.67m in this example. More details of modeling and calculations of this drilled shaft design example are referred to Wang and Cao (2013) and Li et al. (2016b).

Figure 8 shows the variation of D_{min} obtained using the expanded RBD approach with D-method as a function of normalized λ by circles. For each value of normalized λ, Figure 8 also includes D_{min} values obtained using C-method with the exact form (i.e., Eq. (4)) and the approximate form (i.e., Eq. (5)) of variance reduction function by squares and crosses, respectively. The D_{min} values here are determined according to $p_T = 7.2\times10^{-5}$ adopted in Eurocode 7(e.g., Orr and Breysse, 2008). As shown in Figure 8, for a given value of normalized λ , the circle generally plots closely to the squares. The results obtained using C-method with the exact form of the variance reduction function agree well

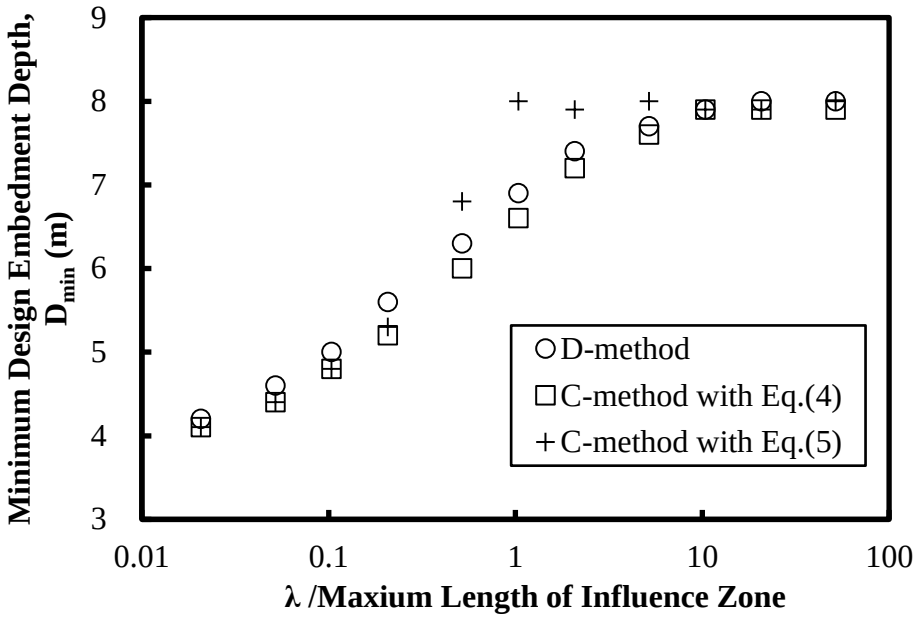

Figure 8 Comparison of sheet pile wall design results using D-method and C-method in expanded RBD

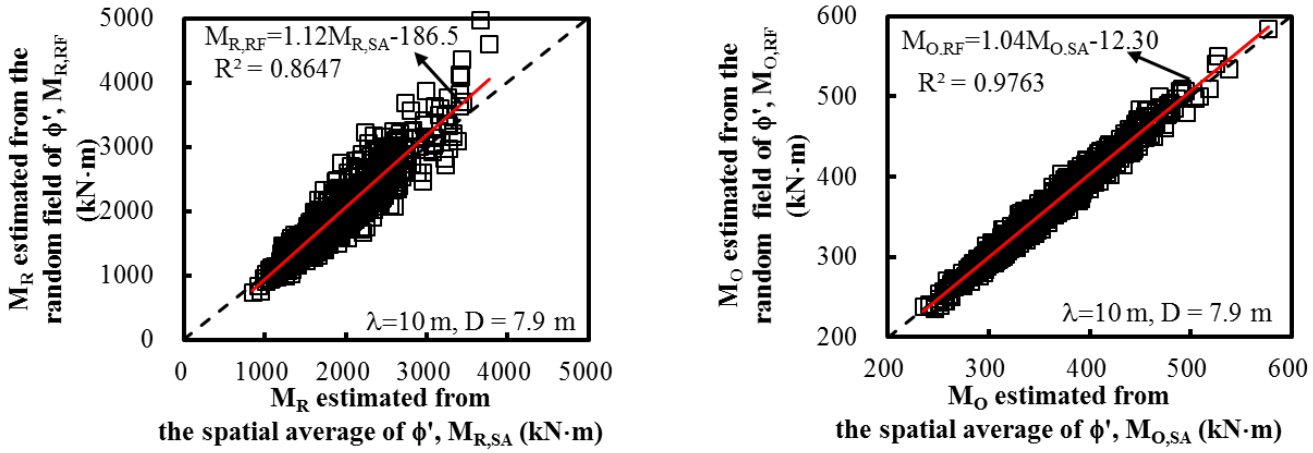

(a) Resistance moment (M_R) (b) Overturning moment (M_O)

Figure 9 Comparison of resistance and overturning moments estimated from realizations of ϕ' random fields and their corresponding spatial averages over influence zones for the design with D=7.9m

with those obtained using D-method. This indicates that spatial averages of ϕ' represents "mobilized" values of ϕ' over the influence zones for M_R and M_O reasonably well in this example. Such an observation is further confirmed by comparing M_R and M_O values estimated from realizations of ϕ' random field in D-method with those calculated from their corresponding spatial averages of ϕ' over influence zones for M_R and M_O, as shown in Figures 9(a) and 9(b), respectively.

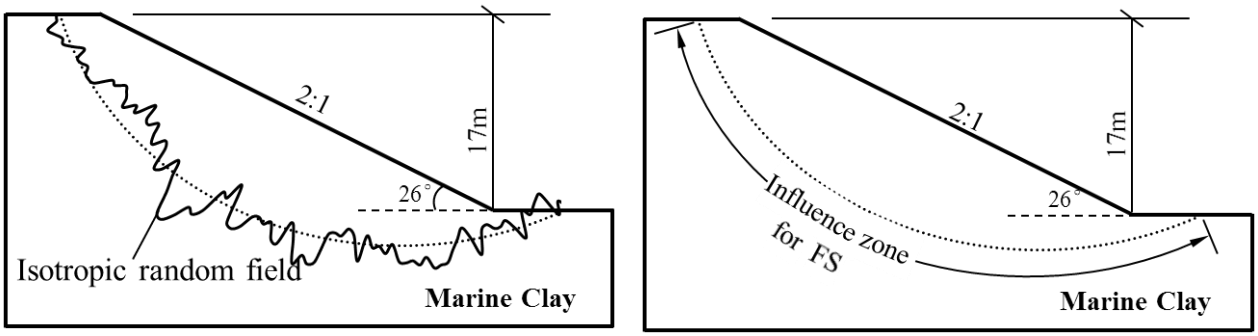

(a) Random field simulation of ϕ' (b) Influence zone for FS

Figure 10 Illustration of spatial variability modeling for Lodalen slide using D-method (see 10(a)) and C-method (see 10(b))

Figure 8 also compares design results obtained from C-method with the exact form (i.e., Eq. (4)) and the approximate form (i.e., Eq. (5)) of variance reduction function. Similar to the drilled shaft design example, when λ is close to L_{max}, there is apparent difference between the two set of design results due to the obvious difference between variance reduction functions calculated from Eqs. (4) and (5) at $\lambda = L_{max}$ (see Figure 3). This, again, indicates that, as the length of influence zone is close to λ adopted in design, using the approximate variance reduction function given by Eq. (5) in C-method may lead to inaccurate design results. Although using Eq. (5) in C-method gives conservative designs in the drilled shaft design example (see Figure 5) and the sheet pile design example (see Figure 8) as λ is close to L_{max}, such an observation cannot be generalized, as illustrated using a soil slope example in the next section.

ILLUSTRATIVE EXAMPLE III: LODALEN SLIDE

This section illustrates effects of using different spatial variability modeling methods (i.e., D-method and C-method) on the "calculated" reliability (or probability of failure) of slope stability using Lodalen slide example. The Lodalen slide occurred in 1954 nearby the Oslo railway station, Norway. As shown in Figure 10, the slope has a height of 17m and a slope angle of 26°. The stratigraphy of slope is comprised of a marine clay layer underlying a 1-m thick clay crust at the top. The clay crust does not significantly affect the stability of the slope (e.g., El-Ramly et al., 2006) and is, hence, not shown in Figure 10. The spatial variability of effective cohesion c', friction angle ϕ' and pore water pressure u in the marine clay layer is considered in this example, and they have respective mean values of 10 kPa, 27.1°, and 0m of water and respective standard deviations of 1.72kPa, 2.21°, and 0.34m of water (e.g., El-Ramly et al., 2006). The correlation structures of the three parameters are considered as identical and are taken as an isotropic single exponential correlation function with a scale of fluctuation λ ranging from 2m to 5000m. More details of the Lodalen slide and its probabilistic assessment (including uncertainty characterization and propagation) are referred to El-Ramly et al. (2006).

For illustration, D-method and C-method are applied to modeling spatial variability of effective shear

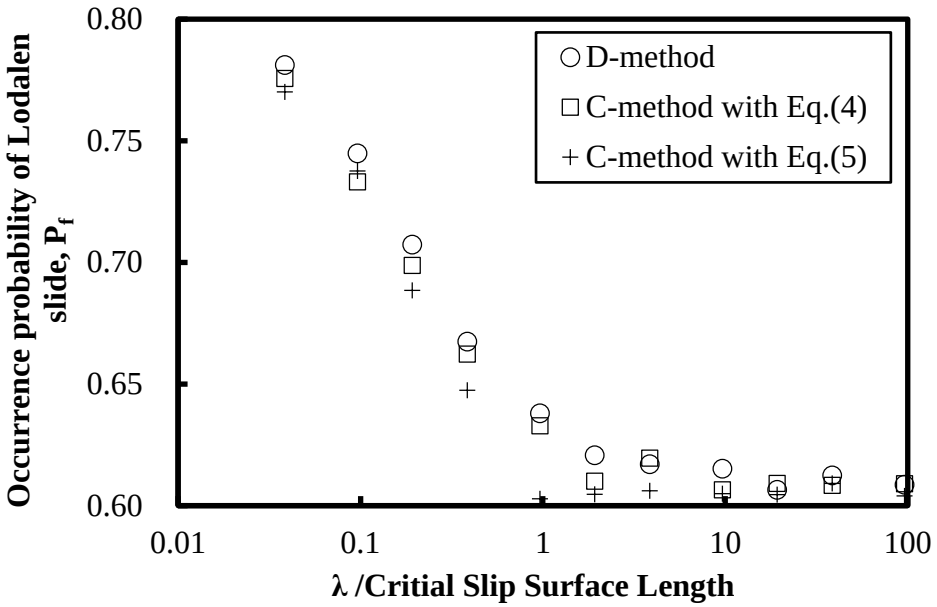

Figure 11 Comparison of occurrence probabilities of Lodalen slide using D-method and C-method in MCS

strength parameters (i.e., c' and ϕ') in the marine clay layer. In this example, the spatial variability of u is always explicitly simulated as a random field by D-method no matter which method is used to modeling spatial variability of c' and ϕ'. Using D-method, random fields of c' and ϕ' can be directly simulated in the marine clay layer without needs of information on the slip surface of Lodalen slide. In contrast, such information is needed for determining the influence zone of sliding resistance of Lodalen slope in C-method. For simplicity, the critical slip surface adopted by El-Ramly et al. (2006) is considered in this report. Then, c' and ϕ' along the critical slip surface are modeled by c'_A and ϕ'_A in C-method, which represent the respective spatial averages of c' and ϕ' over the critical slip surface for evaluating its corresponding FS. The variances of c'_A and ϕ'_A are calculated using their respective variances at the "point" level and the variance reduction function given by Eq. (4) (exact form) or Eq.(5) (approximate form), in which the length of spatial average interval is taken as the length of the critical slip surface, i.e., about 52m in this example. Using D-method and C-method to model spatial variability of c' and ϕ' in the marine clay layer, the occurrence probability P_f of Lodalen slide along the prescribed critical slip surface is calculated for different values of λ varing from 2m to 5000m.

Figure 11 shows the variation of P_f values obtained using D-method as a function of normalized λ by circles. For each value of normalized λ, Figure 11 also includes P_f values obtained using C-method with the exact form (i.e., Eq. (4)) and the approximate form (i.e., Eq. (5)) of variance reduction function by squares and crosses, respectively. It is shown that the circles generally plot closely to the squares. The results obtained using the C-method with the exact form of the variance reduction function agree well with those obtained using D-method. This indicates that the spatial average of effective shear strength of the marine clay represent the "mobilized" value of effective shear strength

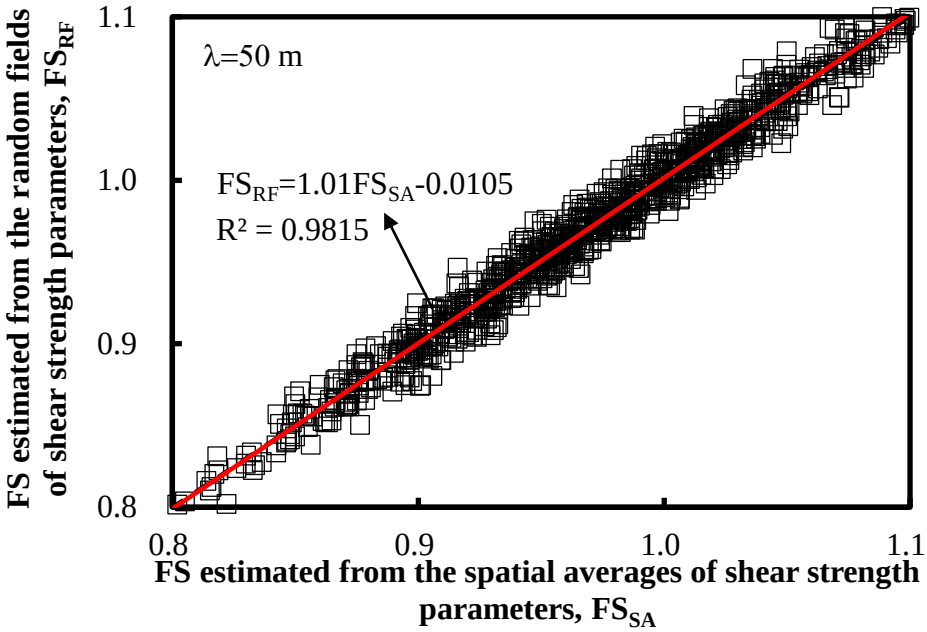

Figure 12 Comparison of safety factors of Lodalen slope calculated from random fields and spatial averages of effective shear strength parameters of the marine clays for λ = 50m

over the critical slip surface reasonably well in this example. Similar to previous two examples, such an observation is further confirmed by comparing FS values estimated from realizations of c' and ϕ' random fields in D-method with those calculated from their corresponding spatial averages over the critical slip surface for a given λ value (e.g., 50m), as shown in Figure 12.

Figure 11 also compares P_f values obtained from C-method with the exact form (i.e., Eq. (4)) and the approximate form (i.e., Eq. (5)) of variance reduction function. When λ is close to the length of the critical slip surface, the crosses plot below the squares, indicating that using the approximate form (i.e., Eq. (5)) of variance reduction function leads to underestimation of P_f at relatively large failure probability levels, which is unconservative. Such unconservative results are attributed to overestimation of variance reduction function by Eq. (5) and, hence, variance of shear strength parameters. This, again, indicates that, as the length of influence zone is close to λ, Eq. (5) shall be used with caution because unconservative reliability estimates might be obtained when it is applied.

SUMMARY AND CONCLUDING REMARKS

This reports summarized major procedures for modeling spatial variability in geotechnical reliability-based design, based on which two methods, so-called decoupled (D)-method and coupled (C)-method are introduced. D-method directly simulates random fields of geotechnical design parameters without considering influence zones and/or critical slip surfaces that affect responses (e.g., resistance moment, bearing capacity, and settlement, etc.) of geotechnical structures. With D-method, ISV modeling is deliberately *decoupled* from geotechnical deterministic analyses. In contrast, C-method uses random

field theory to calculate statistics of spatial averages of geotechnical design parameters within influence zones and/or along critical slip surfaces affecting responses of geotechnical structures. Information on influence zones and critical slip surfaces is needed for calculating statistics of the spatial average of geotechnical design parameters in C-method. Hence, using C-method in geotechnical RBD, ISV modeling is *coupled* with geotechnical deterministic analyses. Based on D-method and C-method, Monte Carlo simulation-based approaches (e.g., expanded RBD) is applied to explore effects of different spatial variability modeling methods on RBD and probabilistic analysis of geotechnical structures, including drilled shaft, sheet pile wall and soil slope. The major conclusions drawn from this study are given below:

(1) Using C-method with exact variance reduction function gives design results and reliability estimates with satisfactory accuracy provided that reasonable influence zones or critical slip surfaces are assumed prior to the analysis. For a given influence zone or critical slip surface, the spatial average serves as a reasonable estimate of "mobilized" shear strength parameters for geotechnical RBD and probabilistic analysis when 1-D spatial variability is considered.

(2) Compared with using exact form of variance reduction function (e.g., Eq.(4)), using approximate form of variance reduction function (e.g., Eq. (5)) in C-methods might lead to conservative or unconservative reliability estimates and design results, depending on the failure probability level. As the length of spatial average interval is close to the scale of fluctuation, Eq. (5) shall be used with particular caution. Note that the effect of the simplified form of variance reduction function can be amplified when 2-D and 3-D spatial variability are considered because reductions in variances of different dimensions are basically "*multiplied*".

(3) Results obtained in this report are preliminary in the sense that failure mechanisms were prescribed prior to the analysis in the three examples and only 1-D spatial variability was taken into account. This is, however, a good starting point to explore the problems concerned in this report for real geotechnical structures, which is beneficial to development of semi-probabilistic geotechnical RBD codes, such as Eurocode 7, and to communication with other research communities with limited background of geotechnical reliability and risk. More rigorous explorations are also warranted that account for effects of different failure mechanisms and 2-D (or 3-D) spatial variability. Some valuable attempts have been made in literature (e.g., Ching and Phoon, 2013; Ching et al., 2014, 2016).

REFERENCES

Baecher, G. B., Christian, J. T., 2003. Reliability and Statistics in Geotechnical Engineering. John Wiley and Sons, New Jersey.

Cao, Z. J., Wang, Y., Li, D. Q., 2016. Quantification of prior knowledge in geotechnical site characterization. Engineering Geology, 203, 107-116.

Cao, Z. J., Wang, Y., 2014. Bayesian model comparison and selection of spatial correlation functions for soil parameters. Structural Safety, 49, 10-17.

Cao, Z. J., Wang, J. M., Wang, Y., 2013. Effects of spatial variability on reliability-based design of drilled shafts. Geotechnical Special Publication: Foundation Engineering in the Face of Uncertainty: Honoring Fred H. Kulhawy, 229, 602-616.

Cao, Z. J., Wang, Y., 2013. Bayesian approach for probabilistic site characterization using cone penetration tests. Journal of Geotechnical and Geoenvironmental Engineering, 139(2), 267-276.

Christian, J. T., Ladd, C. C., Baecher, G. B., 1994. Reliability applied to slope stability analysis. Journal of Geotechnical Engineering, 120 (12), 2180-2207.

Ching, J. Y., Hu, Y. G., Phoon, K. K., 2016. On characterizing spatially variable soil shear strength using spatial average. Probabilistic Engineering Mechanics, 45, 31-43.

Ching, J. Y., Wu, S. S., Phoon, K. K., 2015. Statistical characterization of random field parameters using frequentist and Bayesian approaches. Canada Geotechnical Journal, 53(2), 285-298.

Ching, J. Y., Phoon, K. K., Kao, P. H., 2014. Mean and variance of mobilized shear strength for spatially variable soils under uniform stress states. Journal of Engineering Mechanics, 140(3), 487-501.

Ching, J. Y., Phoon, K. K., 2013. Mobilized shear strength of spatially variable soils under simple stress states. Structural Safety, 41(3), 20-28.

Ching, J. Y., Phoon, K. K., 2012. Probabilistic model for overall shear strengths of spatially variable soil masses. GeoCongress 2012: State of the Art and Practice in Geotechnical Engineering, 2866-2876.

Cho, S. E., 2010. Probabilistic assessment of slope stability that considers the spatial variability of soil properties. Journal of Geotechnical and Geoenvironmental Engineering, 136 (7), 975-984.

Craig, R. F., 2004. Craig's Soil Mechanics. Taylor & Francis, London.

Dasaka, S. M., Zhang, L. M., 2012. Spatial variability of in situ weathered soil. Géotechnique, 62 (5), 375-384.

DeGroot, D. J., Baecher, G. B., 1993. Estimating autocovariance of in situ soil properties. Journal of Geotechnical Engineering, 119(1), 147-166.

El-Ramly, H., Morgenstern, N. R., Cruden, D. M., 2006. Lodalen slide: A probabilistic assessment. Canada Geotechnical Journal, 43(9), 956-968.

El-Ramly, H., Morgenstern, N. R., Cruden, D. M., 2005. Probabilistic assessment of stability of a cut slope in residual soil. Géotechnique, 55(1), 77-84.

El-Ramly, H., Morgenstern, N. R., Cruden, D. M., 2002. Probabilistic slope stability analysis for practice. Canada Geotechnical Journal, 39, 665-683.

Fenton, G., Griffiths, D. V., 2008. Risk Assessment in Geotechnical Engineering. John Wiley and Sons, Hoboken, New Jersey.

Fenton, G. A., Griffiths, D. V., 2007. Reliability-based Deep Foundation Design. Geotechnical Special Publication: Probabilistic Applications in Geotechnical Engineering, 170, 1-12.

Fenton, G. A., Griffiths, D. V., Williams, M. B., 2005. Reliability of traditional retaining wall design. Géotechnique, 55(1), 55-62.

Fenton, G. A., Griffiths, D. V., 2003. Bearing capacity prediction of spatially random c–ϕ soils. Canada Geotechnical Journal, 40 (1), 54-65.

Fenton, G. A., Griffiths, D. V., 2002. Probabilistic foundation settlement on spatially random soil. Journal of Geotechnical and Geoenvironmental Engineering, 128 (5), 381-390.

Fenton, G., 1999a. Estimation for stochastic soil models. Journal of Geotechnical and Geoenvironmental Engineering, 125(6), 470-485.

Fenton, G., 1999b. Random field modeling of CPT data. Journal of Geotechnical and Geoenvironmental Engineering, 125(6), 486-498.

Fenton, G., Vanmarcke, E. H., 1990. Simulation of random fields via local average subdivision. Journal of Engineering Mechanics, 116(8), 1733-1749.

Firouzianbandpey, S., Griffiths, D. V., Ibsen, L. B., Andersen L. V., 2014. Spatial correlation length of normalized cone data in sand: case study in the north of Denmark. Canada Geotechnical Journal, 51(8), 844-857.

Firouzianbandpey, S., Ibsen, L. B., Griffiths, D. V., Vahdatirad, M. J., Andersen L. V., Sørensen, J. D., 2015. Effect of spatial correlation length on the interpretation of normalized CPT data using a kriging approach. Journal of Geotechnical and Geoenvironmental Engineering, 141 (12), 04015052.

Griffiths, D. V., Fenton, G. A., 2009. Probabilistic settlement analysis by stochastic and random finite-element methods. Journal of Geotechnical and Geoenvironmental Engineering, 135 (11), 1629-1637.

Griffiths, D. V., Fenton, G. A., 2004. Probabilistic slope stability analysis by finite elements. Journal of Geotechnical and Geoenvironmental Engineering, 130 (5), 507-518.

Huang, J., Lyamin, A.V., Griffiths, D.V., Krabbenhoft. K., Sloan, S.W., 2013. Quantitative risk assessment of landslide by limit analysis and random fields. Computers and Geotechnics, 53, 60–67.

Huang, J. S., Griffiths, D. V., Fenton, G. A., 2010. System reliability of slopes by RFEM. Soils and Foundations, 50 (3), 343-353.

Jaksa, M. B., 1995. The influence of spatial variability on the geotechnical design properties of a stiff, overconsolidated clay. PHD Thesis of the University of Adelaide.

Jiang, S. H., Li, D. Q., Cao, Z. J., Zhou, C. B., Phoon, K. K., 2015. Efficient system reliability analysis of slope stability in spatially variable soils using Monte Carlo simulation. Journal of Geotechnical and Geoenvironmental Engineering, 141(2), 04014096.

Jiang, S. H., Li, D. Q., Zhang, L. M., Zhou, C. B., 2014. Slope reliability analysis considering spatially variable shear strength parameters using a non-intrusive stochastic finite element method. Engineering Geology, 168, 120-128.

Kulhawy, F. H., 1996. From Casagrande's 'Calculated Risk' to reliability-based design in foundation engineering. Civil Engineering Practice, 11 (2), 45-56.

Li, C. C., Kiureghian, A. D., 1993. Optimal discretization of random fields. Journal of Engineering Mechanics,

119(6), 1136-1154.

Li, D. Q., Xiao, T., Cao, Z. J., Zhou, C. B., Zhang, L, M., 2016a. Enhancement of random finite element method in reliability analysis and risk assessment of soil slopes using Subset Simulation. Landslides, 13, 293-303.

Li, D. Q., Shao K. B., Cao Z. J., Tang, X. S., Phoon, K. K., 2016b. A generalized surrogate response aided-subset simulation approach for efficient geotechnical reliability-based design. Computers and Geotechnics, 74, 88-101.

Li, D. Q., Qi, X. H., Cao Z. J., Tang, X. S., Zhou, W., Phoon, K. K., Zhou, C. B., 2015a. Reliability analysis of strip footing considering spatially variable undrained shear strength that linearly increases with depth. Soils and Foundations, 55(4), 866-880.

Li, D. Q., Jiang, S. H., Cao Z. J., Zhou, W., Zhou, C. B., Zhang, L, M., 2015b. A multiple response-surface method for slope reliability analysis considering spatial variability of soil properties. Engineering Geology, 187, 60-72.

Li, D. Q., Qi, X. H., Phoon, K. K., Zhang, L, M., Zhou, C. B., 2014. Effect of spatially variable shear strength parameters with linearly increasing mean trend on reliability of infinite slopes. Structural Safety, 49, 45-55.

Mitchell, J. K., Soga, K., 2005. Fundamentals of Soil Behavior. John Wiley and Sons, New Jersey.

Orr, T. L., 2015. Risk and reliability in geotechnical engineering. Managing Risk and Achieving Reliable Geotechnical Designs Using Eurocode 7, Chap. 10. Edited by Phoon, K. K., Ching, J. Y., Taylor & Francis CRC Press, 395-433.

Orr, T. L., Breysse, D., 2008. Eurocode 7 and reliability-based design. In Reliability-Based Design in Geotechnical Engineering Computations and Applications, Chap. 8. Edited by Phoon, K. K., London: Taylor & Francis, 298-343.

Phoon, K. K., Huang, S. P., Quek, S.T., 2002. Implementation of Karhunen-Loeve expansion for simulation using a wavelet-Galerkin scheme. Probabilistic Engineering Mechanics, 17(3), 293-303.

Phoon, K. K., Kulhawy, F. H., 1999a. Characterization of geotechnical variability. Canada Geotechnical Journal, 36 (4), 612-624.

Phoon, K. K., Kulhawy, F. H., 1999b. Evaluation of geotechnical property variability. Canada Geotechnical Journal, 36(4), 625-639.

Stuedlein, A. W., Kramer, S. L., Arduino, P., Holtz, R. D., 2012. Geotechnical characterization and random field modeling of desiccated clay. Journal of Geotechnical and Geoenvironmental Engineering, 138(11), 1301-1313.

Tian, M., Li, D. Q., Cao, Z. J., Phoon K. K., Wang, Y., 2016. Bayesian identification of random field model using indirect test data. Engineering Geology, 210, 197-211.

Uzielli, M., Vannuchi, G., Phoon, K. K., 2005, Random field characterization of stress-normalised cone penetration testing parameters. Géotechnique, 55(1), 3-20.

Vanmarcke, E. H., 2010 Random fields: analysis and synthesis. World Scientific.

Vanmarcke, E. H., 1977. Probabilistic modeling of soil profiles. Journal of the Geotechnical Engineering Division, 103 (11), 1227-1246.

Wang, Y., Cao, Z. J., Li, D. Q., 2016. Bayesian perspective on geotechnical variability and site characterization. Engineering Geology, 203, 117-125.

Wang, Y., Cao, Z. J., 2015. Practical reliability analysis and design by Monte Carlo Simulation in spreadsheet. Risk and Reliability in Geotechnical Engineering, Chap. 7. Edited by Phoon, K. K., Ching, J. Y., Taylor & Francis CRC Press, 301-335.

Wang, Y., Cao, Z. J., 2013. Expanded reliability-based design of piles in spatially variable soil using efficient Monte Carlo simulations. Solis and Foundations, 53(6), 820-834.

Wang, Y., 2013. MCS-based probabilistic design of embedded sheet pile walls. Georisk: Assessment and Management of Risk for Engineered Systems and Geohazards, 7(3), 151-162.

Wang, Y., Au, S. K., Kulhawy, F. H., 2011. Expanded reliability-based design approach for drilled shafts. Journal of Geotechnical and Geoenvironmental Engineering, 137(2), 140-149.

Wang, Y., Cao, Z. J., Au, S. K., 2011. Practical reliability analysis of slope stability by advanced Monte Carlo simulations in spreadsheet. Canada Geotechnical Journal, 48 (1), 162-172.

Wang, Y., 2011. Reliability-based design of spread foundations by Monte Carlo simulations. Géotechnique, 61(8), 677-685.

Wang, Y., Au, S. K., Cao, Z. J., 2010. Bayesian approach for probabilistic characterization of sand friction angles. Engineering Geology, 114 (3-4), 354-363.

Xiao, T., Li, D. Q., Cao, Z. J., Au, S. K., Phoon, K. K., 2016. Three-dimensional slope reliability and risk assessment using auxiliary random finite element method. Computers and Geotechnics, 79, 146-158.

Zhang, L. Y., Chen, J. J., 2012. Effect of spatial correlation of standard penetration test (SPT) data on bearing capacity of driven piles in sand. Canada Geotechnical Journal, 49 (4), 394-402.